Optimization of Energy Transfer in a Polymer Composite with Perylene Chromophores

Journal Name

Optimization of Energy Transfer in a Polymer Composite with Perylene Chromophores

Vineeth B. Yasarapudi,[a] Laszlo Frazer,[*a,b] Nathaniel J. L. K. Davis,[c] Edward P. Booker,[d] Alexander Macmillan,[e] Joseph K. Gallaher,[a] Derrick Roberts,[f] Sébastien Perrier,[g] and Timothy W. Schmidt[a]

Luminescent solar concentrators based on molecular dyes are a promising approach to light collection for photovoltaics owing to their potential low cost and wide light acceptance angles. However, they readily suffer from self-absorption, which rapidly reduces device efficiency. We use a perylene-based sensitizer-emitter system to reduce self-absorption. The sensitizer and emitter are copolymerized to enhance energy transfer to the emitter. The sensitizer is susceptible to yield-reducing H-aggregation. We show that a composite polymer can be used to reduce H-aggregation, while maintaining efficient energy transfer.

1 Introduction

Solar energy conversion devices have important economic and environmental benefits. Luminescent solar concentrators[1,2] are a strategy for light collection which could reduce the overall cost of a conversion system. Here, we report methods of increasing the light absorption and emission efficiency of perylene-based luminescent polymers.[3–10]

Primary concerns in the design of luminescent solar concentrators include: a fluorophore absorption spectrum which enables utilization of as much of the solar spectrum as possible, high photoluminescence quantum yield,[11] minimal self-absorption[7] of photoluminescence across a long path length through the concentrator, photostability,[5,6] cost,[12] and finally, waveguiding.[13,14] Efficient waveguiding of luminescence to a device capable of further energy conversion is not considered here. An optimal waveguide would be more cost effective than a mirror-based concentrator because it would collect light incident from a range of angles without moving parts.

For solar concentration applications, perylene derivatives have several advantages. They have a good quantum yield,[1] good photostability,[5,6] and contain the high-abundance elements hydrogen, carbon, oxygen, and nitrogen. However, they absorb in a limited region of the solar spectrum. Owing to overlap between their emission and absorption spectra, they suffer from photoluminescence self-absorption.

To simultaneously broaden the absorption spectrum of the perylene fluorophore and reduce its self-absorption, we used two[15,16] perylene derivatives with different absorption and emission spectra. The structures are shown in in Fig. 1. The perylene with the lower energy singlet excited state serves as the emitter. In a device, the emitter's luminescence will be concentrated. The other perylene, the sensitizer, extends the absorption of the system to higher energies. To reduce self-absorption of emission from the emitter, we use less emitter than sensitizer. We reduce self-absorption of sensitizer emission by transferring the sensitizer energy to the emitter nonradiatively.

Previously, we demonstrated energy transfer from the sensitizer to the emitter through the Förster mechanism.[17] Förster transfer efficiency is highly sensitive to the distance between the sensitizer and emitter.[18] To reduce this distance without creating an excessive concentration of fluorophores, we created a copolymer of sensitizer and emitter, which is illustrated in Fig. 2. The polymer chain covalently maintains the two chromophores in close proximity on dilution. However, not all chains necessarily contain both chromophore types.

A potential downside of a polymer-based approach is that, since the fluorophores are maintained close together, they may have unwanted interactions which reduce the fluorescence quantum yield.[10] For example, an excited fluorophore may form an excimer with its nearest neighbour. These interactions can get stronger if the polymer bends or folds. Previously, we showed that

* Corresponding author E-mail: jmcc@laszlofrazer.com

[a] ARC Centre of Excellence in Exciton Science, School of Chemistry, UNSW Sydney, Australia.

[b] ARC Centre of Excellence in Exciton Science, School of Chemistry, Monash University, Clayton, Australia.

[c] School of Chemical and Physical Sciences, Victoria University of Wellington, Wellington, New Zealand.

[d] Cavendish Laboratory, University of Cambridge, Cambridge, United Kingdom.

[e] Mark Wainwright Analytical Centre, UNSW Sydney, Australia.

[f] Department of Medical Biochemistry and Biophysics, Karolinska Institutet, Stockholm, Sweden.

[g] Department of Chemistry, University of Warwick, Coventry, United Kingdom.
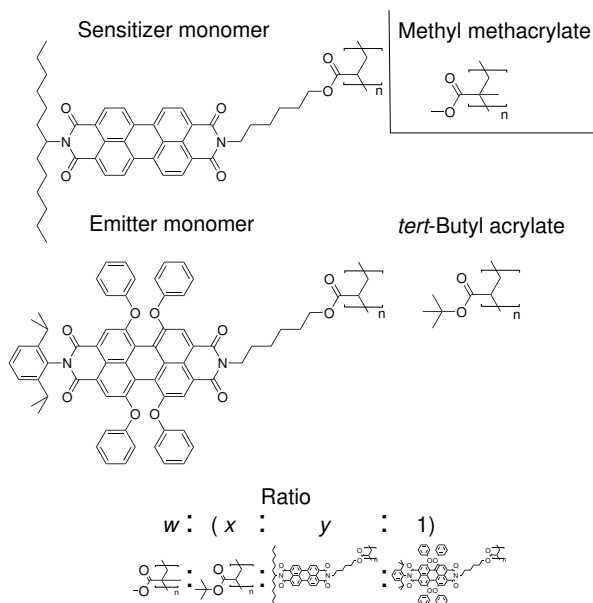
Fig. 1 Structures of the perylene sensitizer, perylene emitter, *tert*-butyl acrylate, and methyl methacrylate units. We copolymerize the sensitizer, emitter, and *tert*-butyl acrylate, but not the methyl methacrylate.
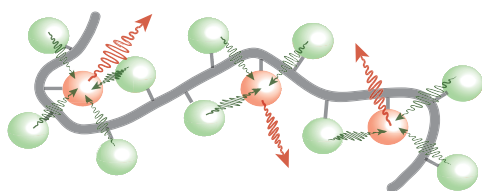

Fig. 2 A cartoon of the solar concentration polymer. The sensitizers (green) absorb sunlight and transfer it to the emitters (red), which emit without self-absorption. Solar concentration can be achieved by placing the polymer in a waveguide (not shown).

Fig. 3 Emission spectrum of the sensitizer polymer (w:(5:1:0)) in a solid solution with PMMA. As the concentration increases, the emission shifts to longer wavelengths, which is characteristic of excimers. The spectra are normalized with respect to the (0,0) peak near 540 nm because this peak is present in each spectrum. See Fig. 11 for the measured quantum yields. 'k' indicates kilo ($\times 10^3$).
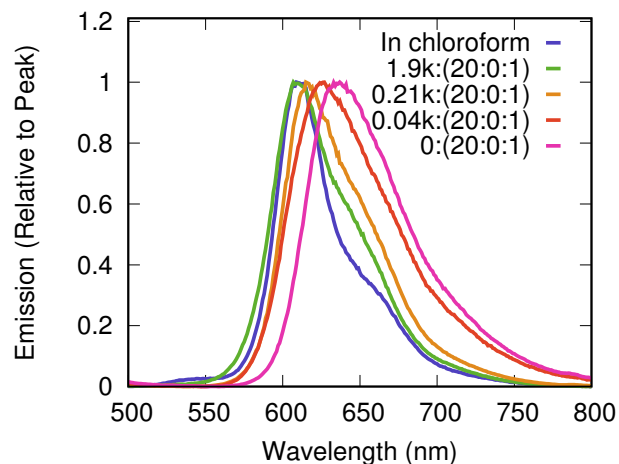
Fig. 4 Emission spectrum of the emitter polymer in a solid solution with PMMA. As the concentration increases, the emission shifts to longer wavelengths, which is characteristic of excitonic coupling. The spectra are normalized with respect to the peak.

the sensitizer monomer quantum yield is 0.91(5) and the emitter quantum yield is 0.90(5).[17] In a hypothetical solar concentrator having noninteracting monomers, a large geometric ratio, quantum yields close to unity, and excessive self-absorption, the primary loss mechanism will be imperfect waveguiding. On self-absorption, the re-emitted fluorescence may not be waveguided. Excimeric losses should be kept small compared to waveguide losses. We show that energy transfer can be maintained while excimers are suppressed.
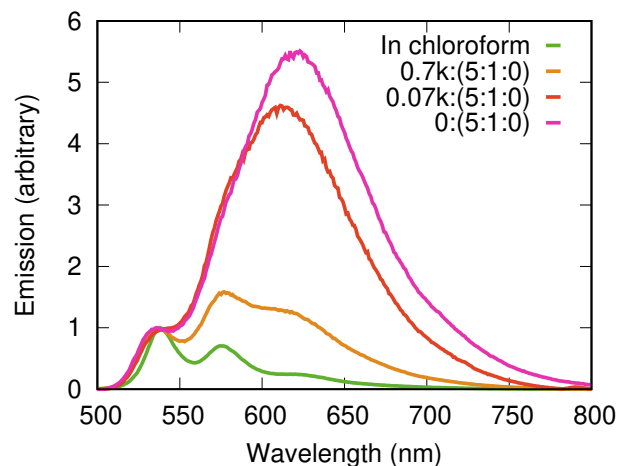

Fig. 5 Absorption (dashed) and emission (solid) spectra of the w:(150:5:1) polymer. Self-absorption decreases for small w. We show that the reduction in sensitizer emission peak (530 nm) is caused by energy transfer.

2   Results & discussion

Fig. 6 Time resolved photoluminescence of the sensitizer polymer (w:(5:1:0)) at 520 nm. As the concentration increases, the initial fluorescence lifetimes decrease because the energy becomes excimers. The excimer lifetime is longer than the fluorescence lifetime. The 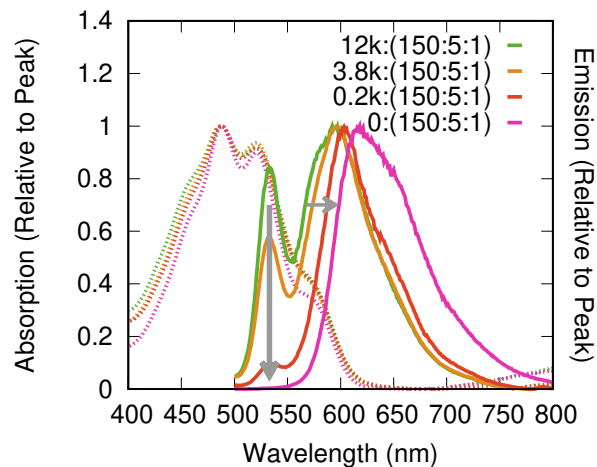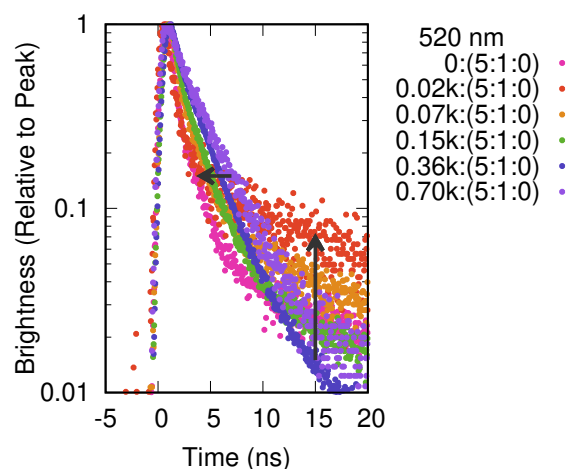presence of excimers results in a longer fluorescence lifetime in the tail of the decay. Arrows indicate the approximate trend caused by increasing concentration.

In order to manipulate the separation among sensitizers and emitters, we use a two-polymer blend to achieve both intrapolymer and interpolymer spacers. The intrapolymer spacer was *tert*-butyl acrylate. The copolymers were prepared with particular molar ratios of *tert*-butyl acrylate to emitter (called x) and sensitizer to emitter (called y). The Poly(methyl methacrylate) (PMMA) acts as the interpolymer spacer. The PMMA is the only species which is not copolymerized. The blend consists of a solid solution of chromophore copolymer in a PMMA matrix. The MMA-to-emitter unit molar ratio is referred to as w, and each sample is described by the formula $w : (x : y : 1)$. In the case where no emitter is present, the formulas are referenced to the number of sensitizers in the format $w : (x : 1 : 0)$. The copolymer molecular weights are not high enough to ensure every polymer chain contains each component.

2.1   H-type aggregation

The steady state emission spectrum of a film of the sensitizer polymer (w:(5:1:0)) shown in Fig. 3 has a pronounced shift to longer wavelengths and broadening compared to the same polymer in solution. This spectral shift is caused by H-type aggregation, which is face-to-face alignment of two chromophores.[19] The film spectrum bears a remarkable resemblance to the excimeric emission spectrum of perylene dimers in solution.[20] The addition of PMMA to the film reduces the H-aggregate contribution to the sensitizer spectrum.
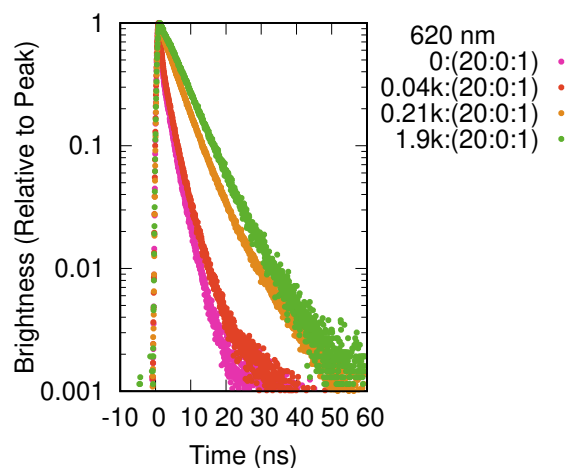
Fig. 7 Time resolved photoluminescence of the emitter polymer at 620 nm. As the concentration increases, the fluorescence lifetime decreases because of self-quenching.
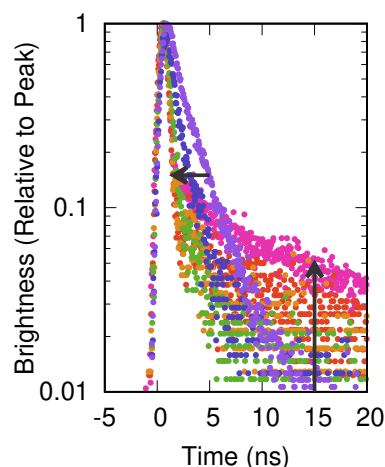
Fig. 8 Time resolved photoluminescence of the (w:(0:5:1)) copolymer at 520 nm. As in Fig. 6, the sensitizer is quenched (arrow towards left) by the formation of a long-lived excimer (upwards arrow).
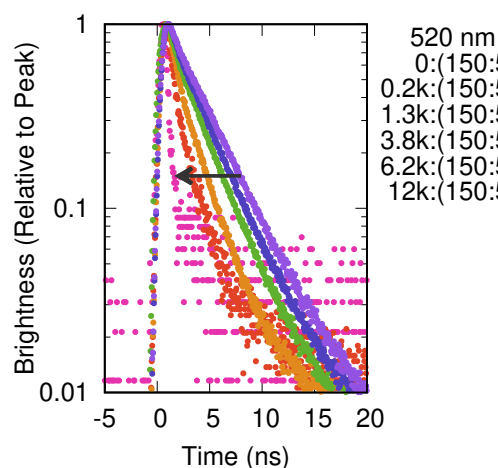
Fig. 9 Time resolved photoluminescence of the (w:(150:5:1)) copolymer at 520 nm. This copolymer shows a similar amount of sensitizer quenching to the copolymer without *tert*-butyl acrylate, but the amplitude of the long-lived excimer is greatly reduced, because the *tert*-butyl acrylate inhibits excimer formation but permits energy transfer to the emitter.

H-type aggregation leads to quenching of the sensitizer fluorescence by excimer formation. Fig. 6 shows that the sensitizer fluorescence at 520 nm decays faster at higher concentrations, because excimers form more easily when sensitizers are close together. The decay of the sensitizer fluorescence is biexponential because it spectrally overlaps the excimer emission. The excimer emission lifetime is long and insensitive to the concentration of the sensitizer. The reduced radiative decay rate is consistent with H-aggregation.[19]

The emitter is functionalised with phenyl groups in the bay position. In addition to shifting the singlet state to lower energy, the functionalisation protects the emitter from aggregation effects.[21] Compared to the sensitizer, the emitter's concentration-dependent spectral shift is much smaller, as shown in Fig. 4. Fig. 7 shows that there is very little long-lived excimer emission in the emitter time resolved emission at 620 nm, but that the emitter lifetime is reduced at high concentration. Singlet fission is a possible contributor to the reduction.[22–25] Since the emitter concentration must be much lower than the sensitizer concentration to produce a low self-absorption device, emitter self-aggregation effects are less important to solar concentrator design.

2.2 Self-absorption performance

The absorption and self-absorption of monomers and polymers with $w = 0$ was previously reported.[17] As a rough estimate of self-absorption which does not depend on the solar concentrator geometry, we calculated the self-absorption ratio as a function of w for the 150:5:1 copolymer. Currie et al. define the self absorption ratio as the molar absorptivity at the absorptivity peak divided by the molar absorptivity at the fluorescence peak.[26] The self-absorption ratio is an imperfect metric. In a well-designed concentrator, the absorptivity at the fluorescence peak will be small. If it is below the noise floor, the self-absorption ratio will be imprecise. In any real solar concentrator the self-absorption depends on the detailed shape of the spectra and on integration over concentrator geometry.[27,28] We would particularly point out in Fig. 5 that the spectrum of the fluorescence peak is bimodal. The sensitizer fluorescence peak is always weaker, so the importance of the successful suppression of sensitizer fluorescence at low w to reducing self-absorption is not reflected in the self-absorption ratio.

Fig. 10 shows that the dilute copolymer (high w) has a similar self-absorption ratio in PMMA and chloroform. However, at high concentrations, H-aggregation shifts the emitter fluorescence to longer wavelengths. Therefore, the absorption at the emission peak diminishes. An increased self-absorption ratio implies that a larger geometric concentration is feasible.

2.2.1 Photoluminescence quantum yield

High photoluminescence quantum yield is a criterion for efficient luminescent solar concentration. Fig. 11 shows that films which have both the in-chain *tert*-butyl acrylate and the interchain PMMA spacers have high quantum yields. The samples were excited so that the sensitizer and emitter molar absorptivity were nearly equal[17], ensuring the contributions of the chromophores to the yield were weighted according to their molar
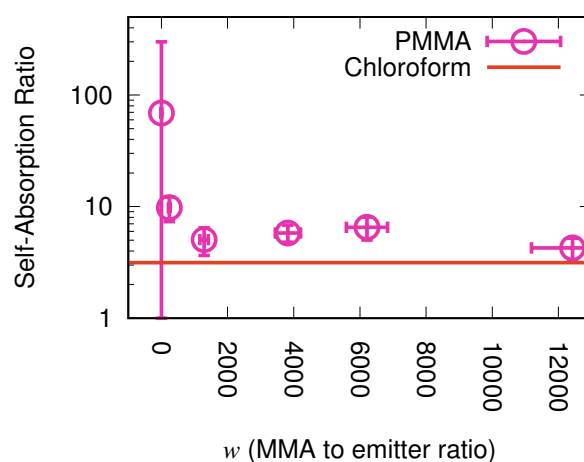

Fig. 10 Self-absorption ratio[26] of the 150:5:1 copolymer in PMMA as a function of concentration. The self-absorption ratio in chloroform is 3.1±0.2 at low concentration.

ratio. Since the films are nonuniform, the measured quantum yields can be viewed as a lower bound. Reabsorption is particularly pronounced in the samples with low PMMA contributions (low w). The results are consistent with the expectation that *tert*-butyl acrylate and PMMA spacers inhibit trap formation.

2.3 Evidence for efficient energy transfer
2.3.1 Reduction of the sensitizer fluorescence lifetime

The fluorescence decay rate of the sensitizer is helpful for measuring the efficiency of energy transfer. In solar concentrators where reduced self-absorption is achieved by radiative transfer[29] to a dilute dopant, the dopant is passive and does not modify the rate constants of the primary fluorophore. We show that our copolymer does not operate like a doped concentrator. Energy transfer to the emitter is driven, not a chance event.

If k_S is the sensitizer radiative fluorescence rate, k_D is the sensitizer dark decay rate, and k_E is the rate of energy transfer from the sensitizer to the emitter, then the energy transfer efficiency is

$$\frac{k_E}{k_E + k_S + k_D}. \tag{1}$$

We measured the total decay rate $k_E + k_S + k_D$ with time correlated single photon counting. Since the sensitizer can form excimers which may result in an increased dark decay rate k_D, an increased total decay rate is not proof of energy transfer, but it is strongly suggestive. In Fig. 6, the sensitizer polymer has $k_E = 0$. Since the total decay rate of the sensitizer in the copolymers in Fig. 9 is greater, despite possessing a lower concentration, k_E is expected to dominate.

Excimers can interfere with energy transfer.[30,31] The excimer radiative decay rate is also variable.[32] Later, we will use excitation-emission spectroscopy to prove that energy is transferred to the emitter; we are able to produce a high total decay rate that is not dominated by dark decay at traps.

In the copolymer with $x = 0$, excimers easily form between sensitizer units because there is nothing to separate them; in the high
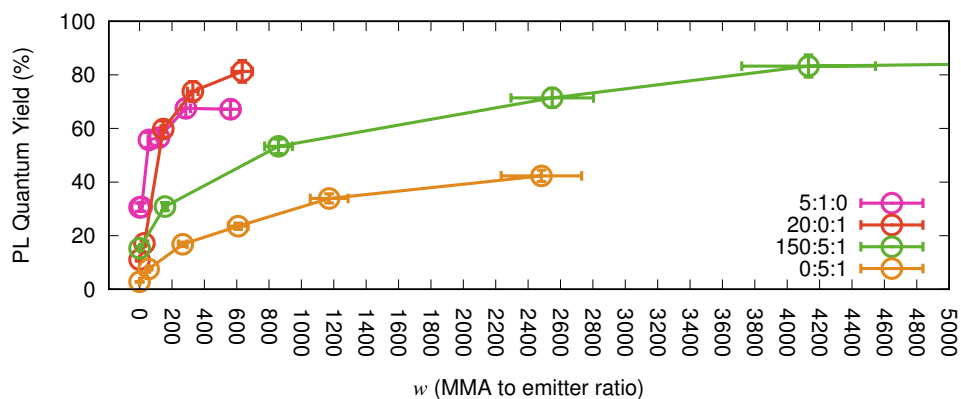
Fig. 11 Photoluminescence quantum yields of films prepared from the four copolymers in various concentrations of PMMA. Excitation 532 nm. Sample self-absorption is nonuniform.

molecular weight limit, there is a 97% chance that the sensitizer has another sensitizer as its nearest neighbour. We assume the polymers form in random order, unlike those of Gutierrez et al.[10] Fig. 8 shows that with $x = 0$, sensitizer fluorescence is quenched to within the instrument response time. However, the presence of PMMA (larger w) can inhibit this quenching. The sensitizer fluorescence for $x = 0$ has a weak but readily detectable biexponential character. We attribute the longer of the two observed lifetimes to a long-lived excimer state. Owing to its lower energy, the excimer is not effectively quenched by the emitter. Its lifetime is not significantly affected by the PMMA concentration w, which should control the sensitizer-emitter transfer rate. For $w = x = 0$, the quenching of the sensitizer is ambiguous: it is caused by a combination of transfer to the emitter and excimer formation. Since the emitter emission is very weak when $w = x = 0$, we conclude trap formation dominates and energy transfer is inefficient.

In the copolymer with $x = 150$, the formation of sensitizer excimers is inhibited because the probability that a sensitizer has another sensitizer as its nearest neighbour is 6% in the high molecular weight limit. We assume again that the polymers form in random order. However, the average number of units between a sensitizer and the nearest emitter is greatly increased, which may inhibit Förster transfer. Nevertheless, we find that the sensitizer is successfully quenched. In Fig. 9, the sensitizer fluorescence lifetime is reduced to near the instrument response for low w, demonstrating sensitizer quenching. The amplitude of the long-lived excimer is reduced by approximately a factor of five. We attribute these results to efficient Förster transfer at high x and low w. Efficient energy transfer will be further supported by the excitation spectra of the samples.

2.3.2 Excitation spectrum of the emitter

Excitation-emission spectra provide a complete picture of the routing of energy from absorption to luminescence in an energy transfer system. In an excitation-emission spectrum, the excitation wavelength indicates where the light was absorbed, if it causes emission. If one species has absorption at that wavelength, and another does not, then the light emitted at that excitation wavelength can be unambiguously assigned to the first species. Likewise, the emission can be assigned to a species.

For solar concentration, the goal is to shift the signal to shorter excitation wavelengths and longer emission wavelengths. When this shift is achieved, self-absorption is reduced because the tail of the absorption overlaps less with the emission. Self-absorption does not always lead to successful recycling[33,34] of a quantum because waveguides possess escape cones. If the luminescence is emitted in the direction of the escape cone, it is not waveguided. Lower self-absorption leads to higher yield because of a reduced chance of loss.

Fig. 12 shows the excitation-emission spectra of the sensitizer and emitter polymers. Since each spectrum contains a single spectroscopically active chemical species, the excitation-emission spectra are in trivial agreement with the one-dimensional absorption and emission spectra. In this figure, the vertically plotted excitation bands of the sensitizer and the horizontally plotted emission band of the emitter are important, because we will show that copolymers with efficient energy transfer combine these two bands.

To show our goal visually, we calculated the idealized excitation-emission spectrum of the sensitizer-emitter copolymer. This is achieved by computing the matrix which is the outer product of two vectors: the sensitizer absorption spectrum and the emitter emission spectrum. Fig. 13 shows the calculated spectrum for perfect energy transfer. This is unrealistic because it assumes the sensitizer is still quenched in the no-emitters limit $y/z \to \infty$. In a realistic solar concentrator, some emitters will be present, so the emission band of the emitter will also show a direct emitter absorption band. To show the impact of aggregation on energy transfer in the excitation-emission spectrum, we show calculations derived from dilute (Fig. 13 a) and concentrated (Fig. 13 b) samples. The sensitizer-emitter interactions are not included in the calculation.

In the dilute sensitizer-emitter polymer, the sensitizer and emitter are spatially separated (12k:(150:5:1)). Therefore energy transfer is reduced. Fig. 14 (a) shows that the dilute sensitizer-emitter polymer excitation-emission spectrum resembles the sum of the sensitizer excitation-emission spectrum and the emitter excitation-emission spectrum, which were presented in Fig. 12. In the dilute sensitizer-emitter polymer, the excitation-emission

(a) Sensitizer
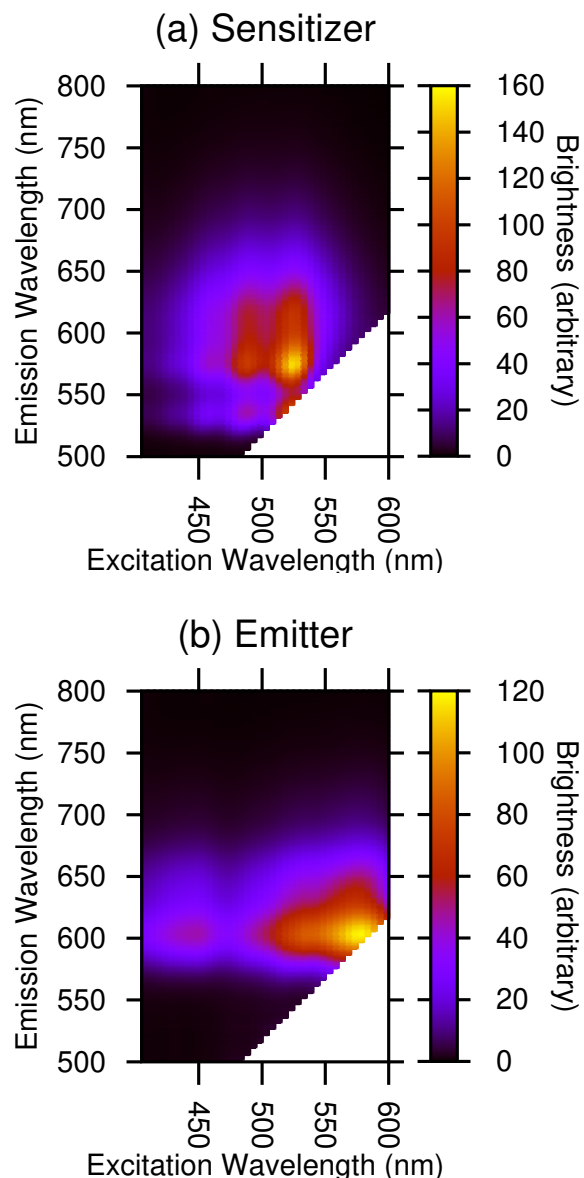
(b) Emitter

Fig. 12 Excitation-emission spectra of the sensitizer 0.7k:(5:1:0) (a) and emitter 1.9k:(20:0:1) (b). The emitter emission occurs and longer wavelengths than the sensitizer absorption, indicating suitability of the system for solar concentration. The white region shows where data was removed because the excitation wavelength was not substantially less than the emission wavelength.

(a) with PMMA

(b) without PMMA

Fig. 13 Model of the contribution of energy transfer to excitation-emission, with (a) and without (b) PMMA.

spectrum shows little energy transfer, in agreement with the time-resolved luminescence measurements.

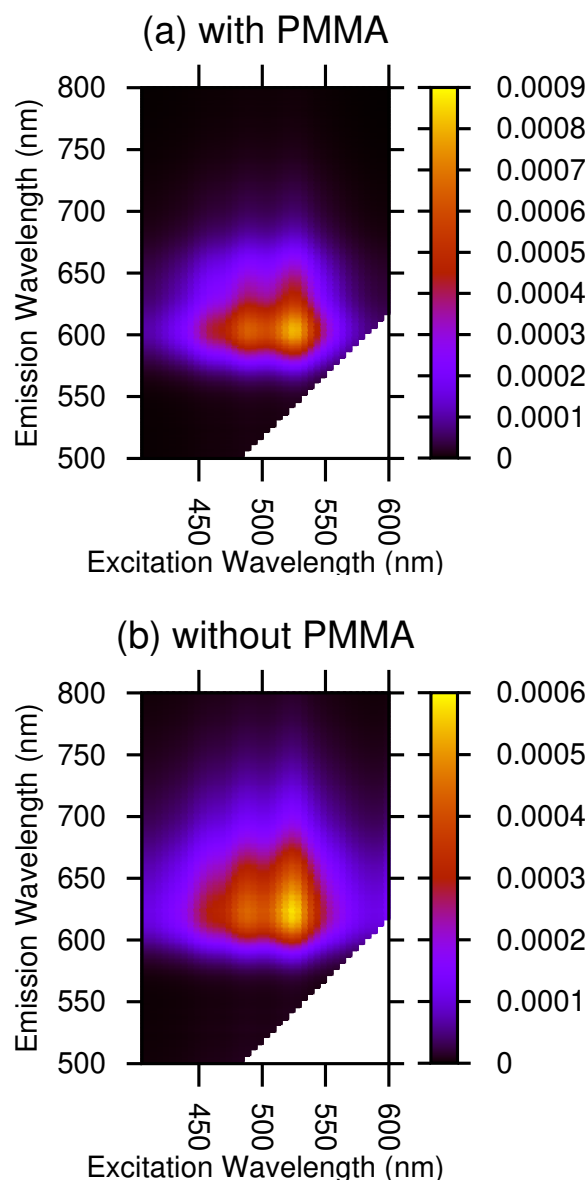Energy transfer becomes apparent in Fig. 14 as the concentration of the copolymer increases. The sensitizer emission band (Fig. 12 (a)) becomes weak relative to the direct emitter emission band in Fig. 14 (c) because the sensitizer is effectively quenched. Near full concentration, the energy transfer signal becomes stronger than the signal from direct excitation of the emitter. Fig. 14 (c) resembles perfect energy transfer modeled in Fig. 13 (a), with the addition of the direct emitter band, which is noticeable at excitation wavelength 575 nm and emission wavelength 600 nm. Ultimately, at full concentration, the emission spectrum is significantly broadened towards the red by excimers.

For the w:(0:5:1) polymer, the excitation-emission experiment is less successful. The direct sensitizer emission is never strong. Neither is the contribution of sensitizer excitation to emitter emission. We conclude that in the absence of *tert*-butyl acrylate, the sensitizer forms excimers which undergo dark decay.

3 Conclusions

Multi-chromophore luminescent solar concentrators face several challenges. We have found that these challenges can be mitigated by designing a composite polymer. As conceptually presented in Fig. 15, if the correct chemical concentrations are selected, improved solar concentration can be achieved.

Using excitation-emission spectroscopy, we have demonstrated that energy was successfully routed from the sensitizer absorption band to the emitter emission band. Since sensitizers outnumbered emitters, and sensitized emission exceeded the direct emission, we conclude that the self-absorption of the luminescent system was successfully reduced.

For both the sensitizer and emitter, H-aggregation is an important issue. While H-aggregation can shift the emission to a longer wavelength, reducing the self-absorption, it also reduces the fluorescence yield below the dilute value.[9,35-38] Our emitter is spectrally shifted by the addition of four phenoxy groups and a diisopropylaniline group. These groups also partially protect the chromophore from H-aggregation. The sensitizer, however, is more prone to H-aggregation. It performs best if partially shielded by two kinds of spacers: an inert intra-polymer *tert*-butyl acrylate spacer and an inter-polymer PMMA spacer. In the future, the effectiveness of our polymer composite strategy could be significantly increased by copolymerizing more perylene sensitizer species,[1] expanding the region of the solar spectrum which is utilized by the concentrator.

4 Experimental

4.1 Materials

We used copolymers consisting of the perylene orange derivative N-(1-hexylheptyl)-N'-(hexylacrylate)perylene-3,4,9,10-tetracarboxylbisimide, the perylene red derivative N-(1-diisopropylaniline)-N'-(hexylacrylate)1,6,7,12-tetra-phenoxy-perylene-3,4,9,10-tetracarboxylbisimide, and *tert*-butyl acrylate. The orange derivative is the sensitizer and the red derivative is the emitter.

The synthesis of copolymers with $x : y : 1$ ratios 20:0:1 and 150:5:1 and NMR methods were previously reported[17] and based on past methods.[39-43] The synthesis of the two copolymers 5:1:0 and 0:5:1 from the previously reported precursors is as follows.

Polymer 0:5:1 – N-(1-hexylheptyl)-N'-(hexylacrylate)perylene-3,4,9,10-tetracarboxylbisimide (78.0 mg, 0.107 mmol), N-(1-diisopropylaniline)-N'-(hexylacrylate)1,6,7,-12-tetra-phenoxy-perylene-3,4,9,10-tetracarboxylbisimide (35.6 mg, 0.0333 mmol) and azobisisobutyronitrile (AIBN) (3.6 mg, 0.022 mmol) in 0.2 mL toluene was degassed via bubbling of N_2 gas. The solution was heated to 70 °C and stirred for 4 h, AIBN (3.1 mg, 0.019 mmol) of was added followed by further degassing and the solution was heated to 70 °C for another 8 h until NMR showed no evidence of acrylate monomer. The crude product was dissolved in THF and precipitated into 0 °C H_2O:MeOH (1:1). The pure product was filtered and dried over phosphoric pentoxide, resulting in 86.1 mg of the pure product. ^{1}H-NMR (CDCl$_3$, 500 MHz): δ = 0.52–0.91 (M, 0.93 H, CH$_3$)), 0.94–1.93 (m, 4.31 H, CH$_2$)), 2.01–2.41 (m, 0.57 H, CH$_2$CH$_2$-N), 3.62–4.24 (m, 0.57 H, CH$_2$N), 4.48–5.17 (m, 0.18 H, COCH$_2$), 6.67–7.49 (m, 0.94 H, benzylic), 7.54–8.87 (m, 1H, perylenes).

Polymer 5:1:0 – N-(1-hexylheptyl)-N'-(hexylacrylate)perylene-3,4,9,10-tetracarboxylbisimide (60.1 mg, 0.0827 mmol), tert-butyl acrylate (44.8 mg, 0.350 mmol) and AIBN (3.3 mg, 0.020 mmol) in 0.2 mL toluene was degassed via bubbling of N_2 gas. The solution was heated to 70 °C and stirred for 5 h, AIBN (3.5 mg, 0.021 mmol) was added followed by further degassing and the solution was heated to 70 °C for another 8 h until NMR showed no evidence of acrylate monomer. The crude product was dissolved in THF and precipitated into 0 °C H_2O:MeOH (1:1). The pure product was filtered and dried over phosphoric pentoxide, resulting in 93.6 mg of the pure product. ^{1}H-NMR (CDCl$_3$, 500 MHz): δ = 0.70–0.95 (M, 1.97 H, CH$_3$)), 1.03–1.88 (m, 79.82 H, CH$_2$)), 2.00–2.47 (m, 7.95 H, CH$_2$CH$_2$-N), 3.87–4.42 (m, 0.94 H, CH$_2$N), 5.11–5.22 (m, 0.36H, COCH$_2$), 8.44–8.82 (m, 1H, perylene).

Table 1 lists the molecular weights of the copolymers. Weights were determined by gel permeation chromatography as previously reported.[17] Only a minority of the sensitizer-emitter copolymer chains contain an emitter; therefore Förster transfer to the emitter is not expected to be efficient at a low concentration of polymers. For solution phase optical spectroscopy, polymers were dissolved in chloroform. All spectroscopic measurements were performed at room temperature (about 23 °C).

Table 1 Average molecular weight and dispersity[44] of each copolymer.

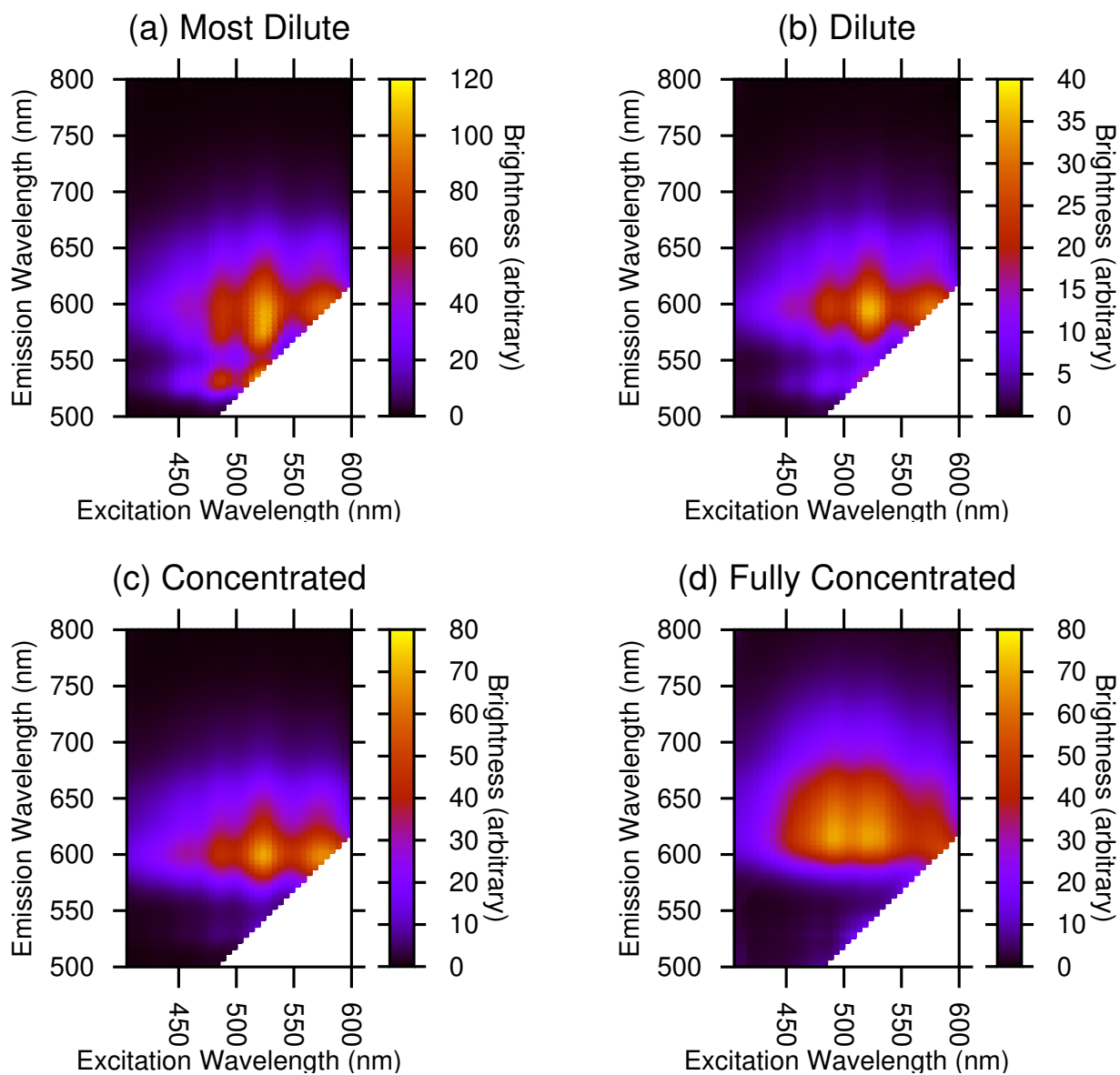| Copolymer	Weight (g/mol)	Dispersity
5:1:0	24306	2.505
20:0:1	3770	5.31
150:5:1	2180	3.22
0:5:1	1839	2.773

Fig. 14 Excitation-emission spectra of the *w*:(150:5:1) copolymer. The dilute sample (a) shows the sensitizer is not quenched. The concentrated sample (c) is similar to the energy transfer model Fig. 13 (a). The fully concentrated sample (d) shows a long-wavelength-shifted spectrum. The formulae are 12k:(150:5:1) (a), 1.3k:(150:5:1) (b), 0.2k:(150:5:1) (c), and 0:(150:5:1) (d).
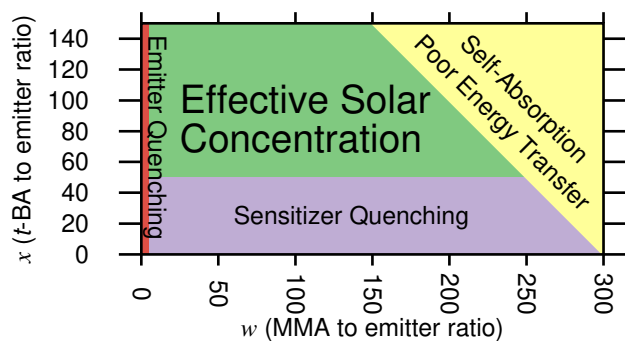
Fig. 15 Illustration of the effect of molar ratios w and x on effective solar concentration in the polymer composite. If the chromophores are too close together, then they can be quenched. If they are too far apart, the transfer from the sensitizer to the emitter is eliminated, so self-absorption dominates. We estimate that the best solar concentration performance is achieved in the green region.

4.2 Film preparation

Paraloid A-11 PMMA was obtained from Rohm and Haas. PMMA is a standard solvent for solid solutions, which is known to have little effect on the fluorescence of isolated perylene fluorophores.[32] Polymer films were fabricated by dissolving a copolymer in chloroform with various concentrations of PMMA. These solutions were dropcast onto glass slides. The volume of the drop was kept constant at 50 μL.

4.3 Absorption spectra

The steady state absorption measurements of liquid solutions were performed with a Cary 100 UV-Vis spectrophotometer. Neat chloroform was used to determine the background for liquid samples. The liquid samples were in a 10 mm path length quartz cuvette.

The absorption spectra of solid films were measured using a Perkin-Elmer Lambda 1050 spectrophotometer including an integrating sphere and photomultiplying detector. The sphere collected light scattered from the rough surface of the films. Since the glass substrates had inconsistent geometry, there is a slight error in the baseline. This was partially corrected by subtracting the absorbance at 675 nm from the spectrum. Uncertainty in the baseline is included in the calculated self-absorption ratios.

4.4 Excitation-emission spectra

Emission and excitation-emission measurements were performed with a Cary Eclipse fluorimeter. The excitation increment was 5 nm. The excitation and emission slit widths were 2.5 nm. A fluorescence cuvette was used for liquid samples and the liquid solutions always had an absorbance less than 0.1. The films were placed at an arbitrary angle to the incident excitation and fluorescence was collected from the back side to reduce scattering. The dropcast films have a nonuniform thickness. As a result, our luminescence measurements of solids may be influenced by self-absorption.

4.5 Luminescence quantum yields

The luminescence quantum yields[45,46] of the sensitizer and emitter in solution were previously reported.[17] Films were placed in an integrating sphere and photo-excited using a 532 nm continuous-wave laser. The laser and the emission signals were measured and quantified using a calibrated Andor Shamrock s4-303i-b spectorgraph and iDus DU490A InGaAs camera for the determination[47] of PL quantum efficiency. The nonuniformity of the films may exacerbate the reabsorption inherent in integrating sphere measurements,[47] so these measurements may be viewed as lower bounds on the internal quantum yield. The excitation was performed so that the molar absorptivities of the sensitizer and emitter were nearly equal.[17]

4.6 Time correlated single photon counting

Broadband time correlated single photon counting measurements were performed using a Horiba Fluoromax. The excitation was performed with a 1 MHz repetition rate, 470 nm laser photodiode. For solid films, the excitation was incident at approximately 45 degrees and the photoluminescence was measured from the back face to reduce laser scatter. The photoluminescence was recorded at a right angle to the excitation using a Czerny-Turner monochromator with an optical grating having 1200 grooves/mm and blazed at 500 nm. The photon count rate was maintained below 1% of the excitation laser repetition rate. Polarization anisotropy was not investigated. The instrument response function full width at half maximum was 1 ns or better.

5 Conflicts of Interest

There are no conflicts of interest to declare.

6 Acknowledgements

References

1 M. G. Debije and P. P. Verbunt, *Advanced Energy Materials*, 2012, **2**, 12–35.

2 W. G. van Sark, K. W. Barnham, L. H. Slooff, A. J. Chatten, A. Büchtemann, A. Meyer, S. J. McCormack, R. Koole, D. J. Farrell, R. Bose *et al.*, *Optics Express*, 2008, **16**, 21773–21792.

3 B. Zhang, H. Soleimaninejad, D. J. Jones, J. M. White, K. P. Ghiggino, T. A. Smith and W. W. Wong, *Chemistry of Materials*, 2017, **29**, 8395–8403.

4 J. L. Banal, H. Soleimaninejad, F. M. Jradi, M. Liu, J. M. White, A. W. Blakers, M. W. Cooper, D. J. Jones, K. P. Ghiggino, S. R. Marder *et al.*, *The Journal of Physical Chemistry C*, 2016, **120**, 12952–12958.

5 G. Seybold and G. Wagenblast, *Dyes and Pigments*, 1989, **11**, 303–317.

6 G. Griffini, L. Brambilla, M. Levi, M. Del Zoppo and S. Turri, *Solar Energy Materials and Solar Cells*, 2013, **111**, 41–48.

7 A. Sanguineti, M. Sassi, R. Turrisi, R. Ruffo, G. Vaccaro, F. Meinardi and L. Beverina, *Chemical Communications*, 2013, **49**, 1618–1620.

8 A. F. Mansour, M. G. El-Shaarawy, S. M. El-Bashir, M. K. El-Mansy and M. Hammam, *Polymer International*, 2002, **51**, 393–397.

9 C. Haines, M. Chen and K. P. Ghiggino, *Solar Energy Materials and Solar Cells*, 2012, **105**, 287–292.

10 G. D. Gutierrez, I. Coropceanu, M. G. Bawendi and T. M. Swager, *Advanced Materials*, 2016, **28**, 497–501.

11 L. Wilson and B. Richards, *Applied Optics*, 2009, **48**, 212–220.

12 D. J. Farrell and M. Yoshida, *Progress in Photovoltaics: Research and Applications*, 2012, **20**, 93–99.

13 M. G. Debije, P. P. Verbunt, B. C. Rowan, B. S. Richards and T. L. Hoeks, *Applied Optics*, 2008, **47**, 6763–6768.

14 C. L. Mulder, P. D. Reusswig, A. M. Velázquez, H. Kim, C. Rotschild and M. Baldo, *Optics Express*, 2010, **18**, A79–A90.

15 A. Taleb, *Renewable Energy*, 2002, **26**, 137–142.

16 R. Ziessel, G. Ulrich, A. Haefele and A. Harriman, *Journal of the American Chemical Society*, 2013, **135**, 11330–11344.

17 N. J. Davis, R. W. MacQueen, D. A. Roberts, A. Danos, S. Dehn, S. Perrier and T. W. Schmidt, *Journal of Materials Chemistry C*, 2016, **4**, 8270–8275.

18 G. D. Scholes, *Annual review of physical chemistry*, 2003, **54**, 57–87.

19 F. C. Spano and C. Silva, *Annual Review of Physical Chemistry*, 2014, **65**, 477–500.

20 J. Sung, A. Nowak-Król, F. Schlosser, B. Fimmel, W. Kim, D. Kim and F. Würthner, *Journal of the American Chemical Society*, 2016, **138**, 9029–9032.

21 Z. Chen, U. Baumeister, C. Tschierske and F. Würthner, *Chemistry-a European Journal*, 2007, **13**, 450–465.

22 A. K. Le, J. A. Bender and S. T. Roberts, *The Journal of Physical Chemistry Letters*, 2016, **7**, 4922–4928.

23 A. K. Le, J. A. Bender, D. H. Arias, D. E. Cotton, J. C. Johnson and S. T. Roberts, *Journal of the American Chemical Society*, 2018, **140**, 814–826.

24 N. Renaud and F. C. Grozema, *The Journal of Physical Chemistry Letters*, 2015, **6**, 360–365.

25 S. W. Eaton, L. E. Shoer, S. D. Karlen, S. M. Dyar, E. A. Margulies, B. S. Veldkamp, C. Ramanan, D. A. Hartzler, S. Savikhin, T. J. Marks *et al.*, *Journal of the American Chemical Society*, 2013, **135**, 14701–14712.

26 M. J. Currie, J. K. Mapel, T. D. Heidel, S. Goffri and M. A. Baldo, *Science*, 2008, **321**, 226–228.

27 J. Batchelder, A. Zewail and T. Cole, *Applied Optics*, 1979, **18**, 3090–3110.

28 J. Batchelder, A. Zewail and T. Cole, *Applied Optics*, 1981, **20**, 3733–3754.

29 B. Swartz, T. Cole and A. Zewail, *Optics Letters*, 1977, **1**, 73–75.

30 R. E. Cook, B. T. Phelan, R. J. Kamire, M. B. Majewski, R. M. Young and M. R. Wasielewski, *The Journal of Physical Chemistry A*, 2017, **121**, 1607–1615.

31 J. Lee, C. Kim, J.-W. Yu, J. Kim, D. Kim, N. Song and C. Kim, *Journal of Polymer Science Part A: Polymer Chemistry*, 2004, **42**, 557–565.

32 M. N. Inci, S. Acikgoz and M. M. Demir, SPIE Photonics Europe, 2016, pp. 988413–988413.

33 L. M. Pazos-Outón, M. Szumilo, R. Lamboll, J. M. Richter, M. Crespo-Quesada, M. Abdi-Jalebi, H. J. Beeson, M. Vrućinić, M. Alsari, H. J. Snaith *et al.*, *Science*, 2016, **351**, 1430–1433.

34 O. D. Miller, E. Yablonovitch and S. R. Kurtz, *IEEE Journal of Photovoltaics*, 2012, **2**, 303–311.

35 J. L. Banal, K. P. Ghiggino and W. W. Wong, *Physical Chemistry Chemical Physics*, 2014, **16**, 25358–25363.

36 J. L. Banal, J. M. White, K. P. Ghiggino and W. W. Wong, *Scientific Reports*, 2014, **4**, 4635.

37 J. L. Banal, J. M. White, T. W. Lam, A. W. Blakers, K. P. Ghiggino and W. W. Wong, *Advanced Energy Materials*, 2015, **5**, 1500818.

38 J. L. Banal, B. Zhang, D. J. Jones, K. P. Ghiggino and W. W. Wong, *Accounts of Chemical Research*, 2017, **50**, 49–57.

39 H. Kaiser, J. Lindner and H. Langhals, *Chemische Berichte*, 1991, **124**, 529–535.

40 Y. Cui, D. Yao, Y. Chen and Z. Wang, *Journal of Polymer Science Part A: Polymer Chemistry*, 2012, **50**, 3485–3492.

41 J. Qu, C. Kohl, M. Pottek and K. Müllen, *Angewandte Chemie*, 2004, **116**, 1554–1557.

42 F. J. Céspedes-Guirao, L. Martín-Gomis, K. Ohkubo, S. Fukuzumi, F. Fernández-Lázaro and Á. Sastre-Santos, *Chemistry-A European Journal*, 2011, **17**, 9153–9163.

43 M. W. Holman, R. Liu and D. M. Adams, *Journal of the American Chemical Society*, 2003, **125**, 12649–12654.

44 J.-M. Lu, M. Wang, Q. Zhang, Z. Li and H. Li, *Chemistry–An Asian Journal*, 2018.

45 A. T. R. Williams, S. A. Winfield and J. N. Miller, *Analyst*, 1983, **108**, 1067–1071.

46 C. Würth, M. Grabolle, J. Pauli, M. Spieles and U. Resch-Genger, *Nature Protocols*, 2013, **8**, 1535.

47 J. C. de Mello, H. F. Wittmann and R. H. Friend, *Advanced materials*, 1997, **9**, 230–232.